

<https://helda.helsinki.fi>

---

# From a Spatial Structure Perspective : Spatial-Temporal Variation of Climate Redistribution of China Based on the Köppen Geiger Classification

Guan, Yanlong

2022-08-16

---

Guan , Y , Liu , J , Wang , K , Cao , W , Jiang , Y , Lu , H & Heiskanen , J 2022 , ' From a Spatial Structure Perspective : Spatial-Temporal Variation of Climate Redistribution of China Based on the Köppen Geiger Classification ' , *Geophysical Research Letters* 15 , e2022GL099319 . <https://doi.org/10.1029/2022GL099319>

---

<http://hdl.handle.net/10138/347187>

<https://doi.org/10.1029/2022GL099319>

---

cc\_by\_nc

publishedVersion

---

*Downloaded from Helda, University of Helsinki institutional repository.*

*This is an electronic reprint of the original article.*

*This reprint may differ from the original in pagination and typographic detail.*

*Please cite the original version.*

# Geophysical Research Letters®



## RESEARCH LETTER

10.1029/2022GL099319

### Key Points:

- A simplified “patch mosaic” model borrowed from landscape ecology was used to assess spatial redistribution of climate zones
- From 1963 to 2098, an apparent signal from fragmentation to aggregation was detected
- Topographic heterogeneity exacerbates the fragmentation of regional spatial structure

### Supporting Information:

Supporting Information may be found in the online version of this article.

### Correspondence to:





J. Liu,  
[junguo.liu@gmail.com](mailto:junguo.liu@gmail.com)

### Citation:

Guan, Y., Liu, J., Wang, K., Cao, W., Jiang, Y., Lu, H., & Heiskanen, J. (2022). From a spatial structure perspective: Spatial-temporal variation of climate redistribution of China based on the Köppen–Geiger classification. *Geophysical Research Letters*, *49*, e2022GL099319. <https://doi.org/10.1029/2022GL099319>

Received 27 APR 2022  
Accepted 6 JUL 2022

## From a Spatial Structure Perspective: Spatial-Temporal Variation of Climate Redistribution of China Based on the Köppen–Geiger Classification

Yanlong Guan<sup>1</sup> , Junguo Liu<sup>1</sup> , Kai Wang<sup>1</sup>, Wenfang Cao<sup>1</sup>, Yelin Jiang<sup>2</sup> , Hongwei Lu<sup>3</sup> , and Janne Heiskanen<sup>4,5</sup>

<sup>1</sup>School of Environmental Science and Engineering, Southern University of Science and Technology, Shenzhen, China, <sup>2</sup>Department of Civil and Environmental Engineering, University of Connecticut, Storrs, CT, USA, <sup>3</sup>Key Laboratory of Water Cycle and Related Land Surface Process, Institute of Geographic Science and Natural Resources Research, Chinese Academy of Science, Beijing, China, <sup>4</sup>Department of Geosciences and Geography, University of Helsinki, Helsinki, Finland, <sup>5</sup>Institute for Atmospheric and Earth System Research, Faculty of Science, University of Helsinki, Helsinki, Finland

**Abstract** Shifting climate zones are widely used to diagnose and predict regional climate change. However, few attempts have been made to measure the spatial redistribution of these climate zones from a spatial structure perspective. We investigated changes in spatial structure of Köppen climate landscape in China between 1963 and 2098 with a landscape aggregation index. Our results reveal an apparent signal from fragmentation to aggregation, accompanied by the intensification of areal dispersion between cold and warm climate types. Our attribution analysis indicates that anthropogenic forcings have a larger influence on changes of spatial structure than natural variation. We also found that topographical heterogeneity is likely to contribute to the regional spatial fragmentation, especially in the Qinghai-Tibet Plateau. However, we also found that the spatial fragmentation will be weakened around the mid-2040s. We argue that biodiversity is likely to be mediated by spatial structure of future climate landscapes in China.

**Plain Language Summary** Shifting climate zones are the most extensively tool for measuring the global and regional climate change, so understanding how they evolve is crucial to improving our ability to diagnose and predict climate change and its potential ecological influences. Previous studies have focused on the area-based shifts between different climate types. However, little attempts have been made to analyze the spatial structure of change in China, simultaneously, causing an apparent gap in the understanding of shifting climate zones. In this study, we investigate changes in the spatial structure of Köppen climate landscape in China between 1963 and 2098 and track its characteristics and driving forces. We reveal an apparent opposite signal from fragmentation to aggregation under SSP5-8.5 scenario. Our attribution analysis indicates that anthropogenic forcings have dominated the evolution of spatial structure over natural ones. Topographical heterogeneity is a well-known factor that exacerbates spatial fragmentation, especially in the Qinghai-Tibet Plateau. We argue that mitigation and adaptation of biodiversity will be regulated by the spatial structural changes of China's climate landscape, and will pose a challenge to biodiversity conservation in the future warming scenario.

## 1. Introduction

Climate is regarded as a more important driver than habitat and topography to explain species spatial extents in the many species distribution models (Luoto et al., 2006; Pecl et al., 2017), especially at the large spatial extents. However, the current comprehensive evaluation of climate change impacts on biomes is not enough or limited due to the lack of available biological data. Different climate classifications are often used to evaluate the influence of climate change on biomes because of strong spatial overlap between climatic boundaries and biomes (Rohli et al., 2015). One of the commonly accepted climate classifications is Köppen–Geiger climate classification first introduced by Köppen (1936). By investigating the moving borders of climate zones, the measurement of novel emergence and disappearing climates has become the most common metric to quantify global and regional climate change (Cui et al., 2021; Garcia et al., 2014).

The availability of large amount of climate data sets enables to diagnose the changes of historical or future Köppen climate zones with their boundaries over China. Earlier research to quantify climate zone change focused on the

© 2022 The Authors.

This is an open access article under the terms of the [Creative Commons Attribution-NonCommercial License](https://creativecommons.org/licenses/by/4.0/), which permits use, distribution and reproduction in any medium, provided the original work is properly cited and is not used for commercial purposes.

area-based shifts between different climate zones (Chan et al., 2016; Huang et al., 2019; Wu et al., 2021). These measurements are extremely important to assess and quantify regional climate change over China. However, due to the spatial heterogeneity of climate patterns at different scales, it should be measured in a variety of ways to close our cognitive gap of climate variability (Garcia et al., 2014). In particular, the geographic migration of species to cooler climates at higher latitudes and higher altitudes has become as one of the most important biological responses (Pecl et al., 2017; Sunday et al., 2012). In the context of global warming, when heterogeneous climatic patches are aggregated or fragmented, not only the composition of the climate landscape, but the spatial structure will also change. This would strongly regulate the redistribution and adaptation of organisms. Moreover, current assumptions about large-scale geographic patterns of species diversity cannot fully interpret global and regional biodiversity patterns (Garcia et al., 2014; Rahbek et al., 2019). In this regard, the measurement of spatial structure can be an important complementary step to estimate the impacts of shifting climate zones on biodiversity.

Under the “patch-mosaic” framework, landscape metrics provide a useful tool to measure changes in the spatial structure of climate landscapes (Guan et al., 2020; McGarigal et al., 2002). Specifically, quantification in spatial structure can not only reflect regional expansion or contraction of climate types (area effects), but can also be used to identify changes that occur at the edges of climate zones that are relatively rich in biodiversity (edge effects) (Laurance, 2004; Maeda et al., 2022). Especially in the mountain regions, it brings starkly distinct climate types close to each other. As the juxtaposition of different climatic zones in mountains disappears, climate types tend to change homogeneously, which will disrupt the balance of climate diversity and species richness, resulting in a decline in biodiversity (Rahbek et al., 2019). From an impact perspective, understanding the spatial structure of China's climate landscape is crucial, and the estimation and projection of spatial fragmentation or aggregation trends can provide new insights into China's ecological conservation plans.

The goal of this study is to determine the spatial changes in terms of aggregation or fragmentation trends in China during 1963–2098 based on the Köppen climate classification. First, we used the observed and simulated data sets to identify the driving force and map Köppen major and sub-climate types. Then, we quantified the area-based standard deviation (SD) change in different Köppen climate types and their links to spatial aggregation changes. Thereafter, we explored the relationships between topographical variables and spatial aggregation changes. Finally, we performed a sensitivity analysis for spatial scales, as well as an analysis of model uncertainty in spatial aggregation. The results on climate landscape of China may provide a new perspective for the formulation and management of biodiversity conservation plans in China.

## 2. Data and Method

### 2.1. Data Sets and Pre-Treatment

The observed ground temperature and precipitation data sets (1961–2014) at  $0.5^\circ \times 0.5^\circ$  grid scale level in China were collected from the National Meteorological Information Center of the China Meteorological Administration (Han et al., 2019). These data sets are generated from about 2400 national meteorological stations, cover most of the land surface in China, and are widely used in the climate research of China.

Temperature and precipitation data for the SSP5-8.5 scenario (2012–2100) were based on the simulations of 13 models (Table S1 in Supporting Information S1) from the Coupled Model Intercomparison Project Phase 6 (CMIP6) (Eyring et al., 2016). SSP5-8.5 was chosen as this scenario represents the most aggressive scenario in fossil fuel use assumed in global climate models, about  $8.5\text{Wm}^{-2}$  relative to pre-industrial conditions at the end of this century. The emissions of SSP5-8.5 are not only consistent with the historical total cumulative  $\text{CO}_2$  emissions, but under current and established policies, are the best match to the projected  $\text{CO}_2$  emissions in the 21st century (Schwalm et al., 2020).

Historical (1961–2014) single-forcing datasets, including CanESM5-CanOE, CESM2, GFDL-CM4, GISS-E2-1-G, MRI-ESM2-0 and MIROC6, were also collected to identify the driving force on spatial structured changes. Specifically, natural-only run (NAT) is an experimental design that is enforced only by natural forcing factors, such as changes in solar irradiance and volcanic activity. In contrast, a well-mixed GHG-only run (GHG) is an experiment with strong anthropogenic influence, enforced only by fully mixed greenhouse gas changes. In addition, a combined historical (ALL) data set of all anthropogenic, natural forcing, and land-use changes was also used to perform the attribution analysis, consisting of the same models (Table S1 in Supporting

Information S1). To maintain consistency of initialization conditions for each model, we chose the uniform ensemble member (r1i1p1f1) in this study (Mahlstein et al., 2013).

Since Köppen–Geiger scheme is sensitive to specific thresholds of temperature and precipitation, the following process was used to reduce biases of simulation data sets. Here, all model outputs were gridded to  $0.5^\circ \times 0.5^\circ$  resolution using bilinear interpolation method. Then a multi-model mean was calculated to reduce the models' uncertainty (Stroeve et al., 2012; Ukkola et al., 2020; You et al., 2021). Additionally, anomalies for the multi-model mean relative to the monthly means was estimated, which was then added to the monthly means of the “base period” of ground temperature and precipitation  $0.5^\circ \times 0.5^\circ$  grid data sets (V2.0) in the time period of 1970–1999 to generate a new climatological temperature and precipitation data set, covering periods from 1961 until 2014 (NAT/GHG/ALL) and from 2012 until 2100 (SSP5-8.5) (Feng et al., 2014; Mahlstein et al., 2013). Considering that the annual climate change will possibly include natural fluctuations of climate zones, a method of 5-year average mean was used to decrease the biases of short-term climate variability, although statistical trends are not highly sensitive to the length of the moving average period (Mahlstein et al., 2013) (Figure S1 in Supporting Information S1). It should be noted that the first and last two years (1961–1962 and 2099–2100) of the time series of the observed and model output will be smoothed out, and data cover period 1963–2098.

Additionally, multiple topographical variables were collected to explore the influence of topographical heterogeneity on spatial structure, including elevation, terrain ruggedness index, roughness and slope with a resolution of  $0.5^\circ$  (Amatulli et al., 2018).

## 2.2. Köppen–Geiger Climate Classification

The Köppen–Geiger climate classification contains 5 major types and 30 subtypes (Table S2 in Supporting Information S1) (Peel et al., 2007). The change of Köppen climate type is dependent on the monthly temperature and precipitation at the grid scale level over mainland China. The annual area percentage of specific climate was estimated by the number of grid boxes. For major types, we considered all climate types, including tropical (A), arid (B), temperate (C), continental (D), and highland (E). For subtypes, since the year-to-year changes in monthly temperature and precipitation will contain large internal variability, we only consider the subtypes with an annual area percentage greater than 5% (total area >95%), including CWA, CFA, DWA, DWB, DWC, BSK, BWK and EF. In addition, we further calculated the cumulative annual changes for each climate types in 1963–2098 relative to the initial year 1963 (5-year average of 1961–1965). On this basis, the SD of the cumulative area change of major and sub-types was further calculated to characterize the mutual transformation characteristics of all climate types.

## 2.3. Landscape Aggregation Index

Quantifying spatial structure of climate zones is important for understanding climate change at a given scale in the context of rapid warming (Garcia et al., 2014). We used the Köppen–Geiger climate classification (Peel et al., 2007) to define climate heterogeneity on the patch scale level. Under the “Patch-Mosaic” paradigm (McGarigal & Cushman, 2005), a climate landscape is denoted as a collection of discrete climatic patches with different temperature and precipitation thresholds. Climatic patches refer to geographic areas with relatively stable hydro-thermal conditions and closed space (Guan et al., 2020; Pickett & Cadenasso, 1995). In Köppen climate landscape of China, all variations are included and quantified based on these climatic patches of different Köppen types. Generally, this paradigm has been verified to be rather effective, which provides a simplifying organizational outline to explore the potential regional climate change from the landscape perspective (Guan et al., 2020). In this study, we chose a landscape aggregation index (AI) to explore the spatial structured change in Köppen climate landscape of China (He et al., 2000). High/low values of AI represent more aggregated/disaggregated pattern of a landscape. The AI of climate type  $i$  in year  $k$  was determined as follows:

$$AI_{ik} = g_{iik} / \max\_g_{iik} \quad (1)$$

where  $g_{iik}$  represents the number of like adjacencies between the grids of climate type  $i$  based on the single-count method in year  $k$  (In the single-count method, each grid adjacency is counted once and the order of grids is not preserved);  $\max\_g_{iik}$  is the maximum number of like adjacencies between the grids of climate type  $i$  based on

the single-count method in year  $k$ . For the year  $k$ , the AI of the total climate landscape pattern depending on the proportion of climate type ( $P_i$ ) and  $g_{ik}$  is calculated as follows,

$$AI_{L,k} = \left[ \sum_{i=1}^I \left( \frac{g_{ik}}{\max - g_{ik}} \right) \times P_{ik} \right] \times 100 \quad (2)$$

On the grid scale level, we further calculated the spatial distribution of AI to explore the relationship between topographical heterogeneity and spatial structured changes. Specifically, taking a moving window square with a slide length of three grid boxes as a small landscape, the calculated value at each small landscape will be returned to the center grid boxes. Each grid box over mainland China will be given a calculated AI value, excluding the three grid boxes at the outermost edge of the grid (null value).

#### 2.4. Attribution and Uncertainty Analysis

To distinguish the influences of natural and anthropogenic forcings on the spatial structure of climate landscape, historical natural (NAT), strong anthropogenic (GHG) single-forcing experiments and mixed historical simulations (ALL) were used for attribution analysis, similar to Yuan et al. (2019). In addition, a non-parametric Mann-Kendall (M-K) statistical test was applied to evaluate the statistical significance of temporal trends (Kendall, 1975; Mann, 1945). Compared to other tests, the M-K significance test is less susceptible to missing values and uneven distribution (Yue et al., 2002).

### 3. Results

#### 3.1. Spatiotemporal Variability of Climate Types in China

Figure 1 show the climatological trends in temperature and precipitation based on observed (1971–2000) and projected (2021–2098) data sets. For temperature, during 1971–2000, most areas show an obvious upward trend ( $>0.05^\circ\text{C}/\text{yr}$ ), excluding Middle Reaches of Yangtze River ( $\sim -0.01^\circ\text{C}/\text{yr}$ ). Especially in the time 2021–2050, the overall temperature increased significantly ( $>0.07^\circ\text{C}/\text{yr}$ ), at the significance level of 0.05 (M-K test). For precipitation, a slight increasing trend is detected in most parts of China during both observed and projected periods. In 1971–2000, the precipitation decreased weakly in the Central China and western Qinghai-Tibet Plateau, while the other regions show an increasing trend. In projected period 2071–2098, the increasing trend of precipitation dominates major parts of China under SSP5-8.5 scenario, while precipitation shows a downward trend in parts of South China.

Compared to precipitation (Figure 1n), the statistical distributions (Figure 1m) show a clear warming trend between 1971 and 2098. In general, the obvious changes in temperature and precipitation will reshape climate landscape patterns of China inevitably between 1963 and 2098. For major types (Figures 1c, 1g and 1k), the notable feature is the expansion and aggregation of continental climate (D), accompanied by the contraction and fragmentation of the highland climate (E) in the Qinghai-Tibet Plateau. For subtypes (Figures 1d, 1h, and 1l), the Qinghai-Tibet Plateau is still the main site for climate type shifts and changes in spatial structure between Ds (i.e., DWB, DWC) and EF.

#### 3.2. Spatial Structured Changes in Climate Landscape

Analyzing changes in areas of the climate types is the basis for assessing changes in the spatial structure of climate landscape. Figures 2a and 2d clearly show an apparent dispersion among cumulative percentage of area changed for Köppen major and sub-types relative to initial year (1963), based on observed and projected data sets. For major types (Figure 2a), the expansion of continental climate type and contraction of highland climate type primarily causes dispersion between 1963 and 2098. Specifically, the area percentage of continental climate (D) increases from  $-0.86\%$  to  $9.97\%$ , while the area of highland climate (E) reduces from  $0.24\%$  to  $-15.74\%$ . For subtypes, the increase of Ds (i.e., DWA, DWC) climate types and decrease of EF causes a similar dispersion trend, compared to that of major types. Specifically, the area percentage of DWA, DWC respectively changed from  $-0.5\%$  to  $9.23\%$  and  $0.2\%$ – $3.8\%$ , while that in DWB and EF reduced from  $-0.73\%$  to  $-4.15\%$  and  $0.36\%$  to



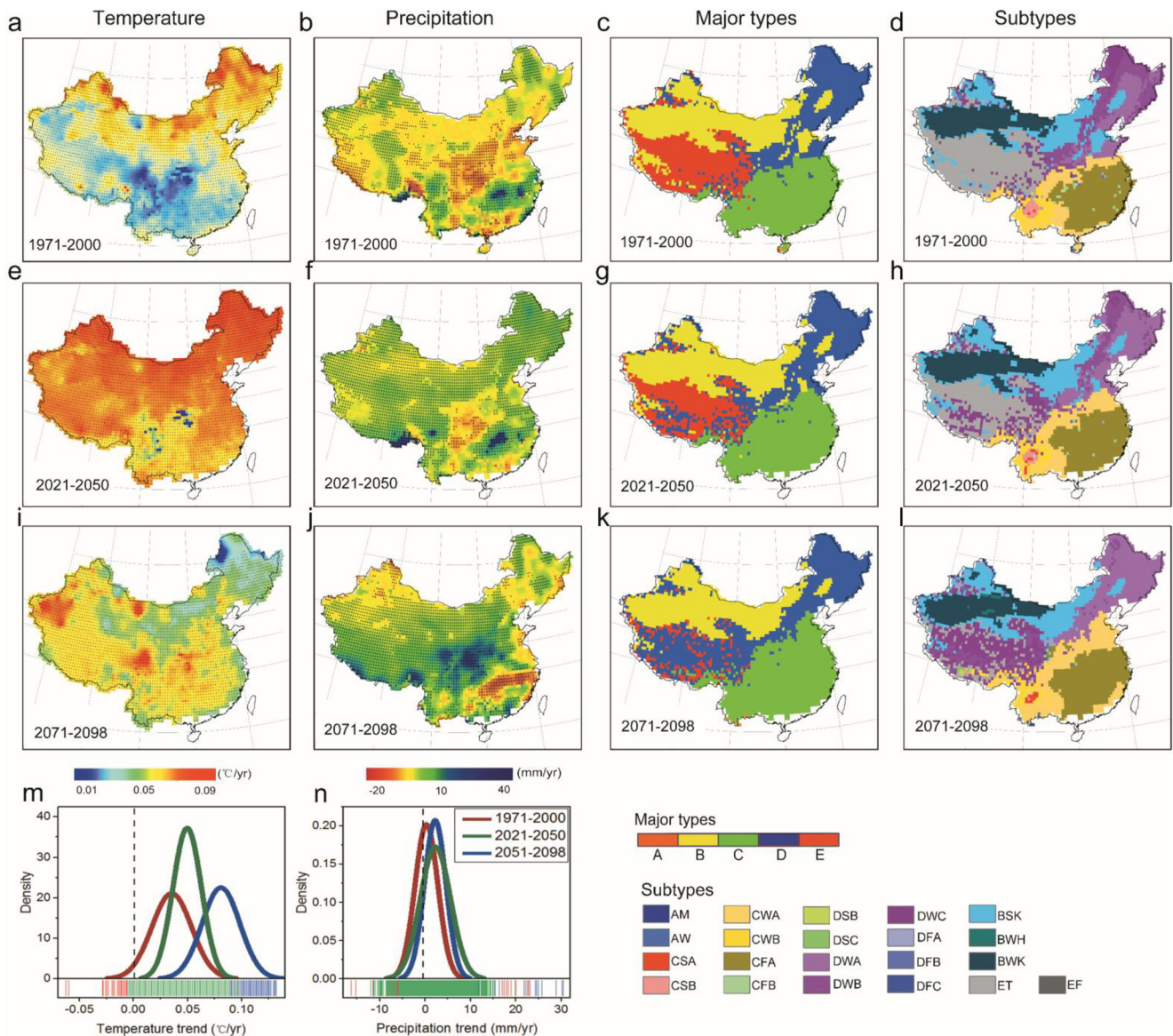


**Figure 1.** Observed and projected trends of (a, e, and i) temperature and (b, f, and j) precipitation, and (m, and n) statistical distributions of trends, as well as, spatial distribution of Köppen (c, j, and k) major and (d, h, and l) sub-types of China for the studied periods (1971–2000, 2021–2050, 2017–2098). Black points represent the significance level of 0.05 (M-K test).

–17.05% by 2098. In general, the intensification of dispersion between warm and cold climate types is an obvious characteristic in Köppen climate landscape of China.

We further calculated the cumulative SD of the major and sub-types to explore the relationship between composition and structure of climate landscape quantitatively. Figures 2b and 2c show that there is a strong response of AI to the intensification of SD among major and sub-types. For major types, SD increased from 0.57% to 11.3% between 1963 and 2098 but AI decreased first and then increased clearly at the range of 87.3% to 86.0%. The inflection point appeared around 2046 and the fitting coefficient of polynomial fit was 0.435 at a significance level of 0.01 (*t*-test). For sub-types, a similar trend was detected as SD intensified with AI decreasing until around 2,047 and then turning to rise at the range of 76.6%–74.4% by 2,098 (*t*-test,  $p < 0.01$ ). In the future warming scenarios, the aggregation trend of subtypes is clearly weaker than that of major types, suggesting that an increase in the number of climate types will reduce the statistical aggregation degree in the climate landscape.

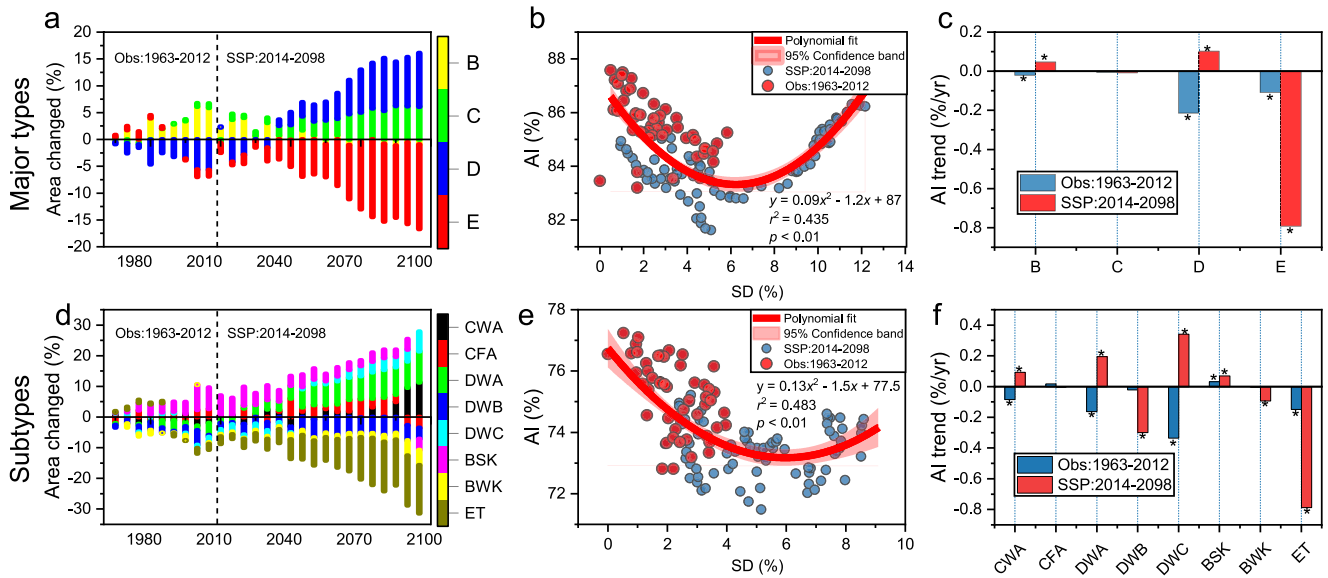


**Figure 2.** Cumulative percentage area relative to 1963 in the Köppen (a) major and (d) sub-types, and (b), (e) polynomial fits between the standard deviation and AI based on observed and projected data sets between 1963 and 2098. (c and f) Temporal trends of AI in the specific Köppen major and sub-types. Red and blue points represent the periods of 1963–2012 and 2014–2098. The asterisk denotes a significance level of 0.01 (M-K test).

Figures 2c and 2f further depict temporal trends of AI in specific major and sub-types. In terms of major types, there is a clear difference in AI between the observed and simulated periods. In 1963–2012, the AI of arid (B), continental (D) and highland (E) types were significantly decreased at the rates of  $-0.02\%/y$ ,  $-0.21\%/y$  and  $-0.1\%/y$  ( $p < 0.01$ , MK). However, in 2014–2098, the AI of B and D is in an obvious increase at the rates of  $0.05\%/y$  and  $0.1\%/y$ , while AI of E decreased rapidly at the rate of  $-0.79\%/y$  ( $p < 0.01$ , MK). In terms of sub-types, in 1963–2012, the AI of CWA ( $-0.08\%/y$ ), DWA ( $-0.16\%/y$ ), DWC ( $-0.33\%/y$ ), BWK ( $-0.09\%/y$ ) and ET ( $-0.15\%/y$ ) decreases, while the AI of CWA ( $0.09\%/y$ ), DWA ( $0.19\%/y$ ), DWC ( $0.34\%/y$ ) and BSK ( $0.07\%/y$ ) increase significantly ( $p < 0.01$ , MK). Overall, between 1963 and 2098, the highland climate type (EF) continued to shrink and fragment, while the warm continental zone (Ds) gradually expanded and aggregated.

### 3.3. Influence of Topographical Heterogeneity on Spatial Structure

Figures 3a and 3d shows that the spatial distribution of AI between the periods of 1971–2000 and 2071–2098 have a clear topographical heterogeneity. Specifically, AI values in Qinghai-Tibet Plateau ( $\sim 20\%$ ) are considerably lower than in other regions. As illustrated in Figures 3c and 3f, there is a clear decreasing trend of gridded AI at the range of 3000–4000 m, which is focused on Qinghai-Tibet Plateau. Figures 3e and 3f further reveals a similar spatial association between topographical variables and AI at the gridded level in China. Specifically, the gridded AI decreased apparently in the west of  $100^\circ\text{E}$  of China between the periods 1971–2000 and 2071–2098. Overall, topographical heterogeneity apparently contributed to regional spatial fragmentation of climate landscape, especially in the Qinghai-Tibet Plateau.

As temperatures rise, even higher-altitude regions cannot remain cold enough to maintain original climate in the future warming scenario. Some cold climates, like EF and ET, will be gradually replaced and dissociated by warmer climate types (Ds), leading to regional fragmentation of climate landscape. Meanwhile, topographic heterogeneity as well-known factor further exacerbates the spatial fragmentation trend, as it can encompass a remarkable volume of different climate types. In particular, many large mountains with high topographic heterogeneity are likely to form many fine-scale microclimates, providing more opportunities for species to mitigate the exposure of climate change. However, as temperatures continue to rise, the spatial structure will tend to aggregate due to enlargement of spatial distribution of warm climate types. When these original cold climates disappear, species endemic to high altitudes will be at risk of extinction.

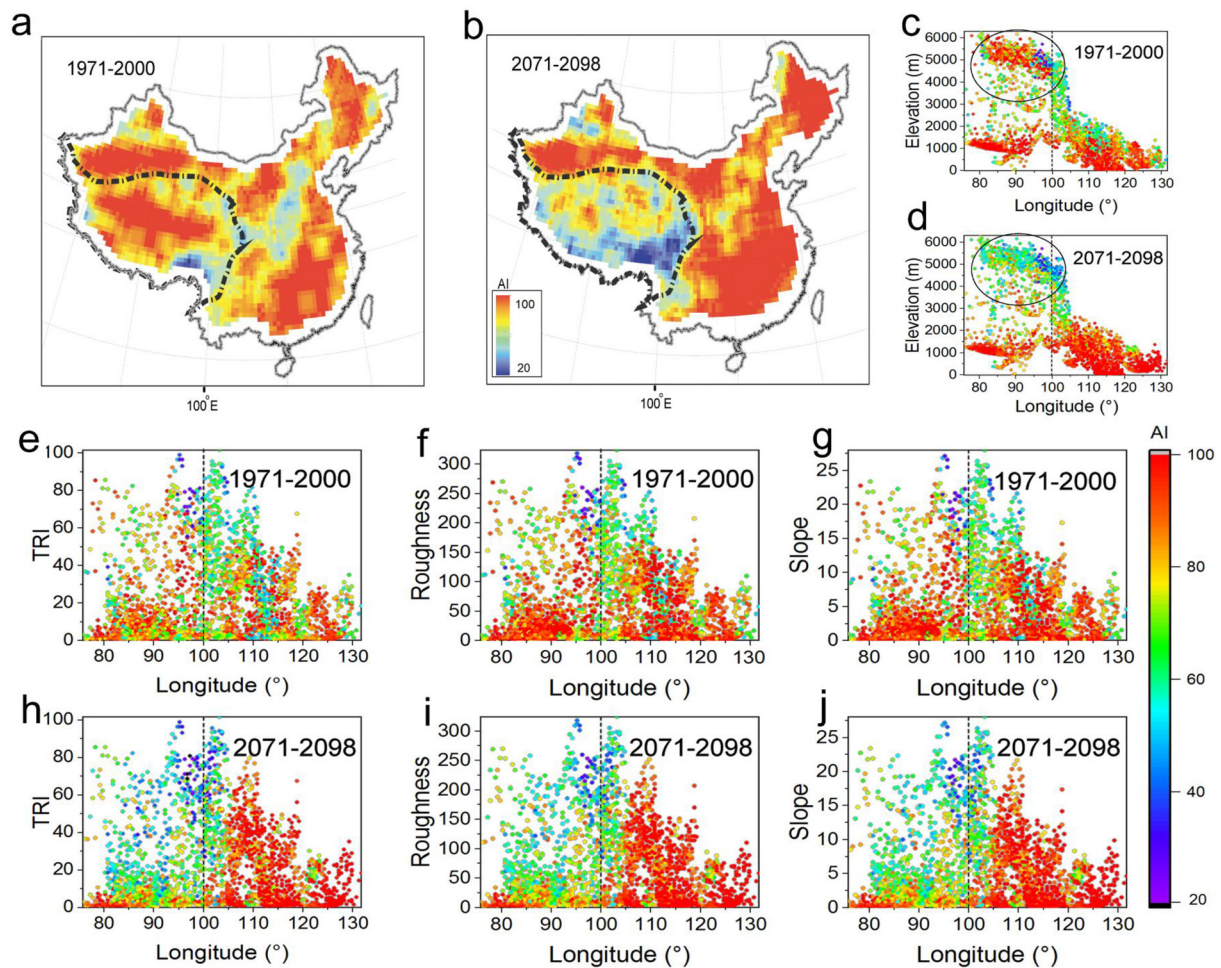


**Figure 3.** AI maps of subtypes in the time (a) 1971–2000 and (b) 2071–2098 based on observed and simulated data sets. Heat maps of (c and d) elevation, (e and h) TRI, (f and i) roughness, (g and j) slope with AI in the time 1971–2000 and 2071–2098.

### 3.4. Attribution and Uncertainty Analysis

Figures 4a and 4d show that the trends of ALL, GHG and Obs ( $-0.07\%/yr$ ) decreased significantly at the major and sub-types (M-K test,  $p < 0.01$ ), while the trends of NAT are in a slight increase at the rates of  $0.08\%/yr$  and  $0.009\%/yr$  for major and sub-types, respectively. Compared with the trends of NAT, the trends of ALL ( $-0.04\%/yr$ ) and GHG ( $-0.03\%/yr$ ) under strong anthropogenic forcings are closer to observed trend (Obs) in 1963–2012. Although these simulations do exhibit quite a large uncertainty, attribution results still clearly reveal that anthropogenic influences should be the driving force of spatial structured changes, rather than natural factors.

Figures 4b and 4e shows the changes of AI and uncertainty of multi-model mean between 1963 and 2098. For major types, the trends are first decreased and then increased around 2047. For sub-types, the AI trend is consistent with that in major types, while the increasing trends are weaker ( $0.003\%/yr$ ) than changes of major types. In terms of uncertainty of simulation results in climate model, future uncertainty (cyan color) tends to increase, especially after the mid-century. Figure S2 in Supporting Information S1 further indicate the distribution of all models, and shows that the multi-model mean can effectively reduce the model error and simulate a consistent and robust AI changes.

Figures 4c and 4f further show the dynamics of AI between different spatial scales for major and sub-types. As the spatial resolution decreased from  $0.1^\circ$  to  $2.0^\circ$ , the spatial aggregation degree of spatial structure decreased obviously, while the downward trends tended to intensify between  $-0.03\%/yr$  and  $-0.08\%/yr$  for major types and between  $-0.03\%/yr$  and  $-0.12\%/yr$  for sub-types. In general, as the spatial resolution decreases, the spatial



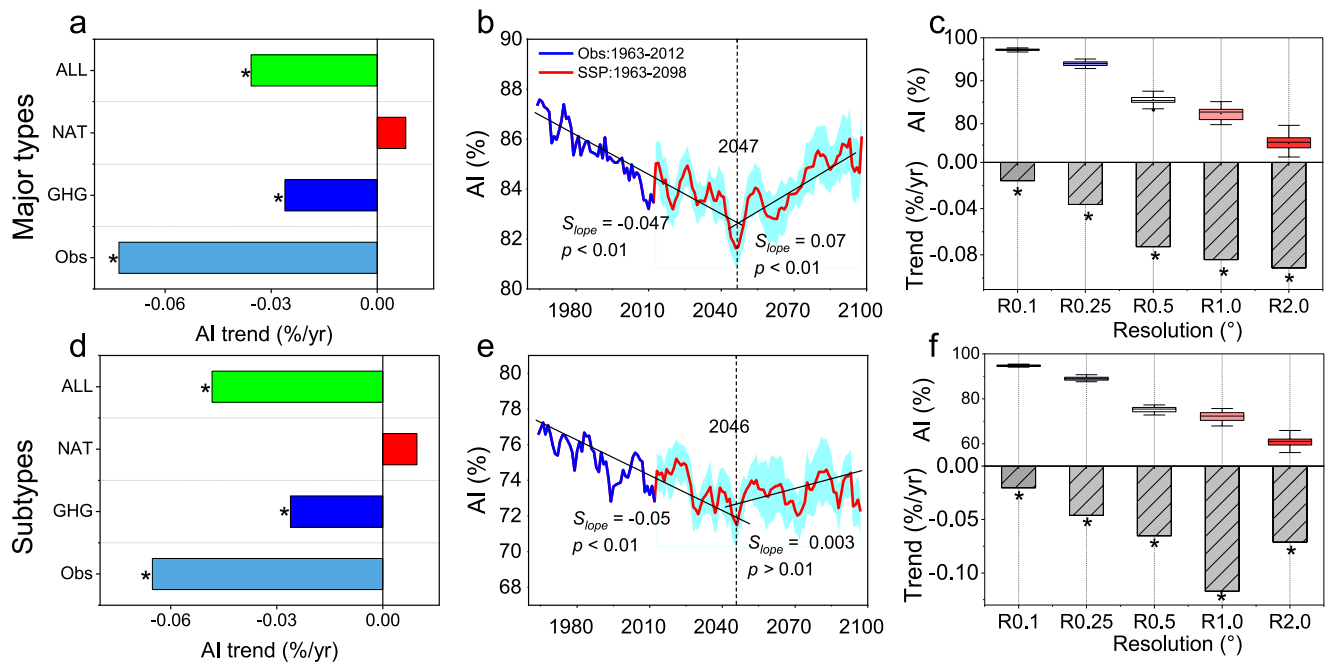


**Figure 4.** Historical attribution analysis based on NAT, ALL and GHG in the Köppen (a) major and (d) sub-types; (b), (e) temporal dynamics from 1963 to 2098 based on observations and SSP5-8.5 simulations. The cyan color denotes  $\pm 1$  s.d. (c), (f) box-charts and trends of different spatial resolutions based on observation during 1963–2012. Abbreviations: ALL, historical simulation with all mixed forcings; NAT, historical simulation but with natural forcing only; GHG, historical simulation but with GHG forcing only; Obs, observation; R0.1-R2.0 represent the different horizontal resolution from 0.1° to 2.0°.

heterogeneity of climate landscape will reduce but the trends will strengthen. However, although there is currently an increasing demand for different models to provide more information at finer spatial resolution, the finer resolution data may detect more small-scale features, making the climate features disordered, requiring further extensive research.

#### 4. Conclusion

The “patch-mosaic” model paradigm provides a simplified framework to assess China's climate change from a spatial structure perspective. Based on observed and projected climate data sets, the spatial structured changes in climate landscape patterns of China were quantified with a landscape AI. Our results show that spatial variations in temperature and precipitation may redistribute the Köppen climate distribution, especially in the future warming scenario. With the intensification of areal dispersion of different climate types, the climate landscape pattern first fragments and then turns to aggregate. We further found that topographical heterogeneity plays an important influence on spatial structure, lowered the regional aggregation, especially in the Qinghai-Tibet Plateau. In addition, our attribution analysis suggests that anthropogenic forcings have a larger impact on spatial structured changes in the climate landscape of China than natural ones. Although the discrepancies of climate models are obvious, most models still simulate a consistent and robust AI change. Characterizing climate landscape can provide a new perspective for the formulation and management of biodiversity conservation plans for future climate change in China.

#### Data Availability Statement

The observed and CMIP6 data sets used in this study are available via <http://data.cma.cn/site/showSubject/id/46.html> (only available in Chinese), and <https://esgf-node.llnl.gov/projects/cmip6/>. The Coupled Model Intercomparison Project Phase 6 models used in this study are listed in Table S1 in Supporting Information S1. Specifically, our data archiving is available at Mendeley via <https://doi.org/10.17632/dzp8hxfmp.1>.

### Acknowledgments

This study has been supported by the National Natural Science Foundation of China (Grant No. 41625001), the Strategic Priority Research Program of the Chinese Academy of Sciences (Grant No. XDA20060402), the Pengcheng Scholar Program of Shenzhen, the Leading Innovative Talent Program for young and middle-aged scholars by the Ministry of Science and Technology, and Guangdong Basic and Applied Basic Research Foundation (2022A1515011070). We are particularly grateful to the two anonymous reviewers and Dr. Olga Hannonen for their useful and careful comments on the manuscript.

### References

- Amatulli, G., Domisch, S., Tuanmu, M. N., Parmentier, B., Ranipeta, A., Malczyk, J., & Jetz, W. (2018). Data descriptor: A suite of global, cross-scale topographic variables for environmental and biodiversity modeling. *Scientific Data*, 5, 1–15. <https://doi.org/10.1038/sdata.2018.40>
- Chan, D., Wu, Q., Jiang, G., & Dai, X. (2016). Projected shifts in Köppen climate zones over China and their temporal evolution in CMIP5 multi-model simulations. *Advances in Atmospheric Sciences*, 33(3), 283–293. <https://doi.org/10.1007/s00376-015-5077-8>
- Cui, D., Liang, S., & Wang, D. (2021). Observed and projected changes in global climate zones based on Köppen climate classification. *Wiley Interdisciplinary Reviews: Climate Change*, 12(3), 1–28. <https://doi.org/10.1002/wcc.701>
- Eyring, V., Bony, S., Meehl, G. A., Senior, C. A., Stevens, B., Stouffer, R. J., & Taylor, K. E. (2016). Overview of the coupled model Inter-comparison Project Phase 6 (CMIP6) experimental design and organization. *Geoscientific Model Development*, 9(5), 1937–1958. <https://doi.org/10.5194/gmd-9-1937-2016>
- Feng, S., Hu, Q., Huang, W., Ho, C. H., Li, R., & Tang, Z. (2014). Projected climate regime shift under future global warming from multi-model, multi-scenario CMIP5 simulations. *Global and Planetary Change*, 112, 41–52. <https://doi.org/10.1016/j.gloplacha.2013.11.002>
- Garcia, R. A., Cabeza, M., Rahbek, C., & Araújo, M. B. (2014). Multiple dimensions of climate change and their implications for biodiversity. *Science*, 344(6183), 1247579. <https://doi.org/10.1126/science.1247579>
- Guan, Y., Lu, H., He, L., Adhikari, H., Pellikka, P., Maeda, E., & Heiskanen, J. (2020). Intensification of the dispersion of the global climatic landscape and its potential as a new climate change indicator. *Environmental Research Letters*, 15(11), 114032. <https://doi.org/10.1088/1748-9326/aba2a7>
- Han, J., Du, H., Wu, Z., & He, H. S. (2019). Changes in extreme precipitation over dry and wet regions of China during 1961–2014. *Journal of Geophysical Research: Atmospheres*, 124(11), 5847–5859. <https://doi.org/10.1029/2018JD029974>
- He, H. S., De Zonia, B. E., & Mladenoff, D. J. (2000). An aggregation index (AI) to quantify spatial patterns of landscapes. *Landscape Ecology*, 15(7), 591–601. <https://doi.org/10.1023/A>
- Huang, W., Yan, J., Liu, C., & Xie, T. (2019). Changes in climate regimes over China based on a high-resolution data set. *Science Bulletin*, 64(6), 377–379. <https://doi.org/10.1016/j.scib.2019.03.001>
- Kendall, M. G. (1975). *Rank correlation methods*. Griffin.
- Köppen, W. (1936). Das geographische system der Klimate. In W. Köppen & G. Geiger (Eds.), *Handbuch der Klimatologie. I. C. Gebr* (pp. 1–44).
- Laurance, W. F. (2004). Forest-climate interactions in fragmented tropical landscapes. *Philosophical Transactions of the Royal Society B: Biological Sciences*, 359(1443), 345–352. <https://doi.org/10.1098/rstb.2003.1430>
- Luoto, M., Virkkala, R., & Heikkinen, R. K. (2006). The role of land cover in bioclimatic models depends on spatial resolution. *Global Ecology and Biogeography*, 16(1), 34–42. <https://doi.org/10.1111/j.1466-822x.2006.00262.x>
- Maeda, E. E., Nunes, M. H., Calders, K., de Moura, Y. M., Raunonen, P., Tuomisto, H., et al. (2022). Shifts in structural diversity of Amazonian forest edges detected using terrestrial laser scanning. *Remote Sensing of Environment*, 271. <https://doi.org/10.1016/j.rse.2022.112895>
- Mahlstein, I., Daniel, J. S., & Solomon, S. (2013). Pace of shifts in climate regions increases with global temperature. *Nature Climate Change*, 3(8), 739–743. <https://doi.org/10.1038/nclimate1876>
- Mann, H. B. (1945). Nonparametric tests against trend. *Econometrica: Journal of the Econometric Society*, 13(3), 245–259. <https://doi.org/10.2307/1907187>
- McGarigal, K., & Cushman, S. A. (2005). The gradient concept of landscape structure. *Issues and Perspectives in Landscape Ecology*, 112–119. <https://doi.org/10.1017/CBO9780511614415.013>
- McGarigal, K., Cushman, S. A., Neel, M. C., & Ene, E. (2002). FRAGSTATS: Spatial pattern analysis Program for categorical maps (pp. 1–182). [https://doi.org/10.1016/S0022-3913\(12\)00047-9](https://doi.org/10.1016/S0022-3913(12)00047-9)
- Pecl, G. T., Araújo, M. B., Bell, J. D., Blanchard, J., Bonebrake, T. C., Chen, I. C., et al. (2017). Biodiversity redistribution under climate change: Impacts on ecosystems and human well-being. *Science*, 355(6332). <https://doi.org/10.1126/science.aai9214>
- Peel, M. C., Finlayson, B. L., & McMahon, T. A. (2007). Updated world map of the Köppen-Geiger climate classification. *Hydrology and Earth System Sciences*, 11(5), 1633–1644. <https://doi.org/10.5194/hess-11-1633-2007>
- Pickett, A. S. T. A., & Cadenasso, M. L. (1995). Landscape ecology: Spatial heterogeneity in ecological systems. *Science*, 269(5222), 331–334. <https://doi.org/10.1126/science.269.5222.331>
- Rahbek, C., Borregaard, M. K., Colwell, R. K., Dalsgaard, B., Holt, B. G., Morueta-Holme, N., et al. (2019). Humboldt's enigma: What causes global patterns of mountain biodiversity? *Science*, 365(6458), 1108–1113. <https://doi.org/10.1126/science.aax0149>
- Rohli, R. V., Joyner, T. A., Reynolds, S. J., & Ballinger, T. J. (2015). Overlap of global Köppen-Geiger climates, biomes, and soil orders. *Physical Geography*, 36(2), 158–175. <https://doi.org/10.1080/02723646.2015.1016384>
- Schwalm, C. R., Glendon, S., & Duffy, P. B. (2020). RCP8.5 tracks cumulative CO<sub>2</sub> emissions. *Proceedings of the National Academy of Sciences of the United States of America*, 117(33), 19656–19657. <https://doi.org/10.1073/PNAS.2007117117>
- Stroeve, J. C., Kattsov, V., Barrett, A., Serreze, M., Pavlova, T., Holland, M., & Meier, W. N. (2012). Trends in Arctic sea ice extent from CMIP5, CMIP3 and observations. *Geophysical Research Letters*, 39(16). <https://doi.org/10.1029/2012GL052676>
- Sunday, J. M., Bates, A. E., & Dulvy, N. K. (2012). Thermal tolerance and the global redistribution of animals. *Nature Climate Change*, 2(9), 686–690. <https://doi.org/10.1038/nclimate1539>
- Ukkola, A. M., De Kauwe, M. G., Roderick, M. L., Abramowitz, G., & Pitman, A. J. (2020). Robust future changes in meteorological drought in CMIP6 projections despite uncertainty in precipitation. *Geophysical Research Letters*, 47(11), 0–3. <https://doi.org/10.1029/2020GL087820>
- Wu, B., Lang, X., & Jiang, D. (2021). Köppen climate zones in China over the last 21,000 years. *Journal of Geophysical Research: Atmospheres*, 126(6). <https://doi.org/10.1029/2020JD034310>
- You, Q., Cai, Z., Wu, F., Jiang, Z., Pepin, N., & Shen, S. S. P. (2021). Temperature dataset of CMIP6 models over China: Evaluation, trend and uncertainty. *Climate Dynamics*, 57(1–2), 17–35. <https://doi.org/10.1007/s00382-021-05691-2>
- Yuan, X., Wang, L., Wu, P., Ji, P., Sheffield, J., & Zhang, M. (2019). Anthropogenic shift towards higher risk of flash drought over China. *Nature Communications*, 10(1), 1–8. <https://doi.org/10.1038/s41467-019-12692-7>
- Yue, S., Pilon, P., Phinney, B., & Cavadias, G. (2002). The influence of autocorrelation on the ability to detect trend in hydrological series. *Hydrological Processes*, 16(9), 1807–1829. <https://doi.org/10.1002/hyp.1095>